after sample collection, after equilibrium weight was attained for each filter stored in desiccators at constant relative humidity of ca. 40% under 295 ± 3 K, resulting in 14 ± 6 mg (mean $\pm$ S.D., $n = 36$). All the QFF samples were stored at 253 K until subjected to the exposure experiments or analysis.

2.4 *Passive exposure of OHNPs to indoor air on QFF and on airborne particles*

Ten pmol of 3-, 6- and 8-OHNPs dissolved in methanol were uniformly deposited on a QFF directly by the following procedure: 2 mL of the stock solution (5 nM) was evenly dribbled onto the QFF with a microsyringe, and then the solvent was evaporated at room temperature in the dark. The air-dried QFF was passively exposed to indoor air containing trace levels of O_3 (less than 1 ppbv) for 1 and 18 hours in the dark at room temperature. In order to avoid interference of OHNPs originally contained in the airborne particulate samples with the HPLC analysis, 10 pmol of 3-OHNP-d_8 dissolved in methanol was deposited onto airborne particles collected on a QFF as described above. 3-OHNP-d_8 adsorbed on airborne particles was also exposed to indoor air for 24 hours according to the same procedure. The remaining OHNPs and 3-OHNP-d_8 were analysed by HPLC after extraction from the QFF or airborne particle samples as described above.

2.5 *Active exposure of 3-OHNP-d_8 to ambient air on airborne particles under the high volume air sampling condition*

Decomposition of 3-OHNP-d_8 on airborne particles during high volume air sampling was evaluated according to the following procedure. Ten pmol of 3-OHNP-d_8 and 1-NP-d_9, which was added in order to determine the recovery during the sample pretreatment, dissolved in methanol were uniformly deposited on airborne particles that were collected on a QFF as described above. After being installed in a high volume air sampler, the QFF was exposed to ambient air containing up to 60 ppbv of O_3 at a flow rate of 1500 L min^{-1} for 1–9 hours. The remaining 3-OHNP-d_8 and 1-NP-d_9 were analysed by HPLC after extraction from the airborne particles as mentioned above. To clarify the unexpected formation of 3-OHNP-d_8 by oxidation of 1-NP-d_9 during the high volume air sampling, the active exposure of 1-NP-d_9 in the flow system was also performed independently.

2.6 *Airborne particle collection for the determination of the atmospheric particle-associated OHNPs with the correction method*

TSP were collected every 3 hours at the same site, as is described in Section 2.3. Sampling was conducted using a high-volume air sampler with a QFF at a flow rate of 1500 L min^{-1} during 26–27 November 2001 for 24 hours. A total of 8 samples were prepared. The filter samples onto which 0.5 mL of 10 nM 3-OHNP-d_8 solution was added as an internal standard were subjected to the extraction process.

2.7 *Measurement of gases*

The concentration of O_3 in the air was monitored using a UV spectrophotometric O_3 analyser (Dylec, Model 1150) or obtained by public environment monitoring stations in Sakai, Osaka, Japan.

3. Results

3.1 *Chemical analysis of OHNPs by HPLC*

HPLC chromatograms of authentic and extracted OHNPs from airborne particles are shown in Figure 1(a) and (b), respectively. 3-, 6-, and 8-Hydroxy-1-aminopyrenes (3-, 6-, and 8-OHAPs) and 3-OHAP-d_8, which are the reduced compounds of the corresponding OHNPs, were successfully detected with good separation for each peak by a HPLC/chemiluminescence detection system. Figure 1(c) shows a chromatogram of an SOF sample analysed by the HPLC/chemiluminescence detection system without the reducer column in the system. In the case without the reduction, the OHAP peaks were completely eliminated from the chromatogram because OHNPs were not reduced into their corresponding fluorescent OHAPs in the HPLC system. After washing the SOF with 5% NaOH/water, the peaks derived from acidic OHNPs having phenolic hydroxyl groups also disappeared from the chromatogram (Figure 1(d)). These results ensure that the peaks, the retention times of which are consistent with those of the authentic OHAPs, originate from OHNPs that have nitro and phenolic hydroxyl groups in their structures.

3.2 *Passive exposure of OHNPs to indoor air on QFF and airborne particles*

Figure 2 shows the time course of the remaining fractions of OHNPs directly deposited on QFF, i.e. OHNPs on the 'naked' QFF, during passive exposure to indoor air. The mean OHNP recoveries from unexposed filters (exposure time: 0 h) were 70–85%. The mean recoveries of OHNPs after passive exposure to indoor air for 1 and 18 hours were 26–38 and 2–5%, respectively. No significant difference in the degradation was observed among the three OHNP isomers at the same exposure time. In addition, it was possible to uniquely identify 3-OHNP-d_8 from the peaks of OHNP isomers originally contained in ambient airborne samples using the HPLC system. Hereafter, therefore, we evaluated the degradation for 3-OHNP-d_8 as a representative OHNP. The loss of 3-OHNP-d_8 deposited on airborne particles, i.e. 3-OHNP-d_8 on the 'particle-loaded' QFF, was not significant even after 24 hours of exposure (mean recovery $\pm$ S.D.: $79 \pm 12\%$, $n=4$) in the passive mode.

3.3 *Active exposure of 3-OHNP-d_8 to ambient air on airborne particles during high volume air sampling*

Figure 3 shows the recovery of 3-OHNP-d_8 from the airborne particles after active exposure to the ambient air for 1–9 hours. The mean concentrations of O_3 during the exposures were not entirely identical. The recovery of 1-NP-d_9 was stable during the exposure to ambient air under the high volume sampling condition (mean recovery $\pm$ S.D.: $93 \pm 10\%$, $n=25$). In contrast, 3-OHNP-d_8 was easily decomposed in the active mode even on the airborne particles. The mean recovery of 3-OHNP-d_8 was less than 20% after 9 hours of exposure. Formation of 3-OHNP-d_8 by oxidation of 1-NP-d_9 on the airborne particles was not observed in the active mode.

4. Discussion

O_3 is one of the most powerful oxidants in the atmosphere. The effect of O_3 concentration on the loss of PACs under high volume air sampling conditions has been investigated

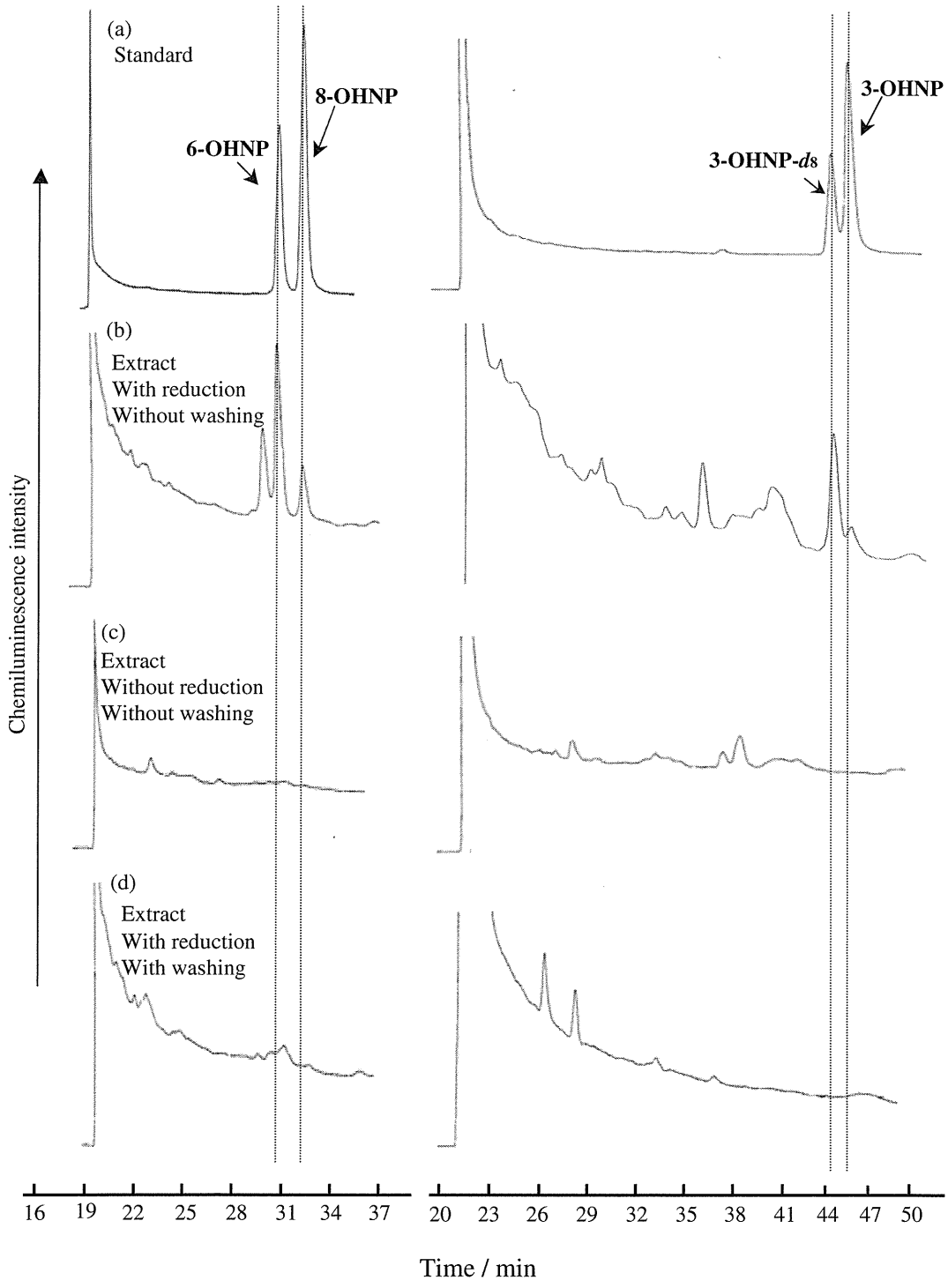

Figure 1. Typical chromatograms from the HPLC-chemiluminescence detection system for standard solution of 6-, 8-, and 3-OHNPs and 3-OHNP-d_8 (internal standard) and soluble organic fraction (SOF) of airborne particles. OHNPs were reduced into their corresponding amino compounds in the HPLC system, and then were detected by the chemiluminescence detector. (a) Authentic standard of the OHNPs, (b) SOF of airborne particles, (c) SOF of airborne particles without the reduction process, (d) SOF of airborne particles with washing process with 5% NaOH solution. In the case without the reduction or with the washing process, the peaks of the compounds were eliminated from the chromatograms (see text for details). Amounts of authentic OHNPs determined: 268 fmol (3-OHNP); 230 fmol (6-OHNP); 335 fmol (8-OHNP); 183 fmol (3-OHNP-d_8). Amounts of OHNPs from the SOF: 35 fmol (3-OHNP); 239 fmol (6-OHNP); 70 fmol (8-OHNP). Quantification limit of the HPLC system employed for each OHNP was 2 fmol (S/N = 10). Injection volume: 20 µL.

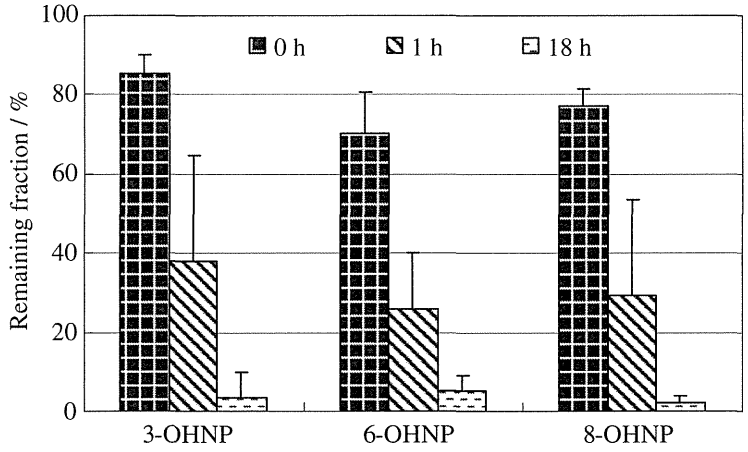

Figure 2. Decays of the remaining fractions of OHNPs directly deposited on quartz fibre filters during passive exposure to indoor air. Error bars represent one standard deviation of the average ($n=3$, 10, and 8 for 0, 1, and 18 h exposure, respectively).

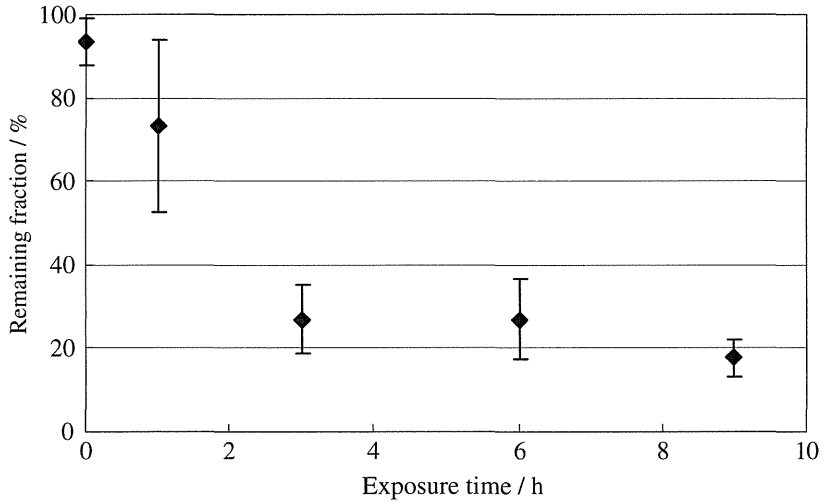

Figure 3. Decays of the remaining fractions of 3-OHNP-d_8 on airborne particles deposited on quartz fibre filters under the high volume air sampling condition at various O_3 concentrations. Data are represented as the mean $\pm$ S.D. ($n=3$ except for 0 and 1 h exposure; $n=4$ and 12 for 0 and 1 h exposure, respectively).

in numerous studies, and the lifetime or residual fraction of the PACs was found to be inversely correlated with O_3 concentration [8,20,21]. The decomposition of 3-OHNP-d_8 on airborne particles during high volume air sampling was also strongly expected to be attributable to oxidation reactions by O_3, although a possibility of contribution of other atmospheric oxidants such as OH and NO_3 radicals to the chemical degradation of 3-OHNP-d_8 can not be completely excluded. In this study, therefore, we evaluated the relationship between the degradation of 3-OHNP-d_8 on airborne particles and O_3 flux (N_{O3}/molecules min^{-1}). This was calculated from the mean concentration of O_3 in the ambient air and the flow rate during the air sampling.

Figure 4 shows the dependence of N_{O3} on the remaining 3-OHNP-d_8 on the airborne particles deposited on the QFF after 1 hour of active exposure. The recovery of 3-OHNP-d_8 from airborne particles clearly decayed with increasing N_{O3} ($r=0.91$, $p<0.01$).

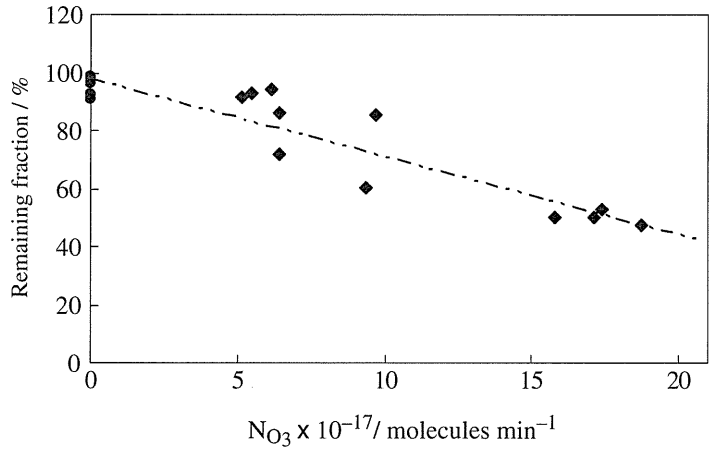

Figure 4. Remaining fraction of 3-OHNP-d_8 deposited on airborne particles after 1 h of exposure to ambient air under the high volume air sampling condition plotted against gas phase O_3 flux; number of molecules passing through the quartz fibre filter per minute (N_{O3}/molecules min^{-1}). The remaining fractions of 3-OHNP-d_8 at 0 molecules min^{-1} of N_{O3} were obtained from the 3-OHNP-d_8 recoveries from unexposed airborne particles to ambient air (circles).

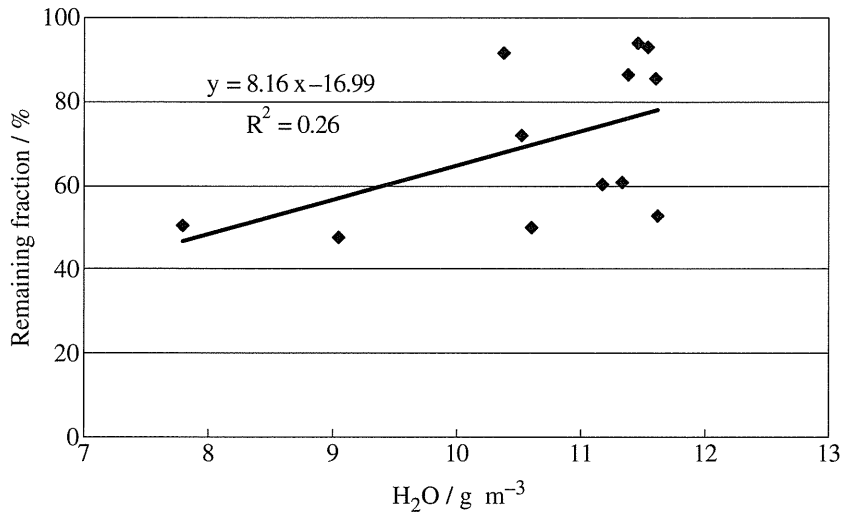

Figure 5. Plot of remaining fraction of 3-OHNP-d_8 on airborne particles deposited on quartz fibre filters after 1 h of active exposure versus water vapour concentration in ambient air.

The loss of PAHs on atmospheric soot particles with respect to the effects of humidity and ambient temperature have been evaluated previously [22]. In the present study, a clear relationship between the humidity in the ambient air and the remaining fraction of 3-OHNP-d_8 on QFF during high volume air sampling was not observed (Figure 5). Contrariwise, the recovery of 3-OHNP-d_8 increased with decreasing ambient temperature during the air sampling (Figure 6). The data points were classified into three categories according to N_{O3} as shown in Figure 6. Both the remaining 3-OHNP-d_8 fraction and the inverse of the temperature seem to be low in the high N_{O3} group, but clear temperature dependence on the remaining 3-OHNP-d_8 was not observed within each N_{O3} category. The O_3 concentration in the atmosphere was usually high in the daytime when the ambient temperature and solar intensity were also high because of active photochemical

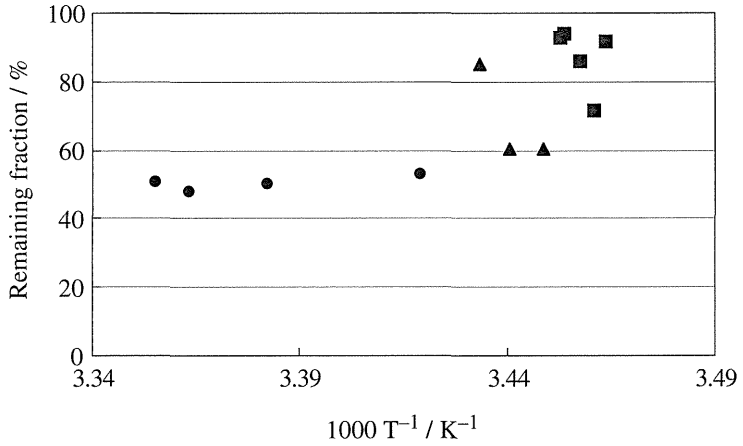

Figure 6. Plot of remaining fraction of 3-OHNP-d_8 on airborne particles deposited on quartz fibre filters after 1 h of active exposure under various O_3 flux (N_{O3}) conditions versus inverse of ambient temperature: circles, $N_{O3} = (15.8–18.7) \times 10^{17}$ molecules min^{-1}; triangles, $N_{O3} = (9.35–9.68) \times 10^{17}$ molecules min^{-1}; squares, $N_{O3} = (5.16–5.48) \times 10^{17}$ molecules min^{-1}.

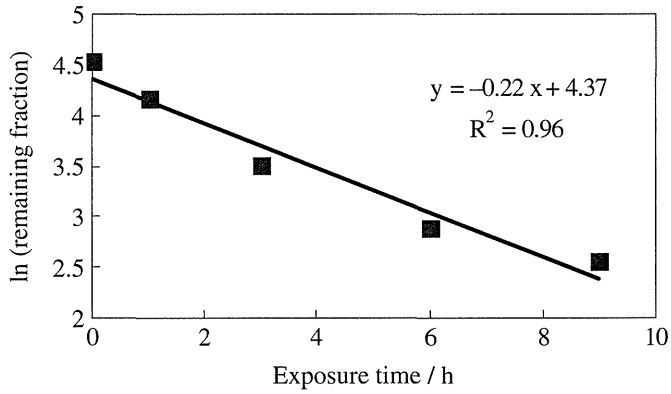

Figure 7. Logarithmic decay of 3-OHNP-d_8 exposed to ambient air under the high volume air sampling condition at 1.0×10^{18} molecules min^{-1} of O_3 flux (N_{O3}, mean $N_{O3} \pm$ S.D.: $(1.0 \pm 0.1) \times 10^{18}$ molecules min^{-1}). The time-dependence decay displays clear single exponential behaviour.

reactions contributing to O_3 formation. The result obtained implies that there is no significant relationship between the ambient temperature and the remaining 3-OHNP-d_8 during high volume air sampling. A similar result was observed in the previous report [8].

In order to understand the relationship between OHNP degradation and exposure time at the same O_3 concentration, the results obtained under the N_{O3} of 1.0×10^{18} molecules min^{-1} are shown in Figure 7. A linear relationship was observed between the logarithm of the residual fraction of 3-OHNP-d_8 and exposure time under similar N_{O3} conditions ($r^2 = 0.96$, $p < 0.01$), indicating a first-order reaction with respect to 3-OHNP-d_8 concentration. Therefore, the pseudo-first-order reaction constant for the decay of 3-OHNP-d_8 deposited on the airborne particles on QFF can be obtained for each exposure assuming a constant N_{O3}. Perraudin *et al.* [23] also reported that the plots for the reaction of PAHs adsorbed on different types of particles with O_3 exhibit an exponential decay over time under constant O_3 concentration and determined the pseudo-first-order rate

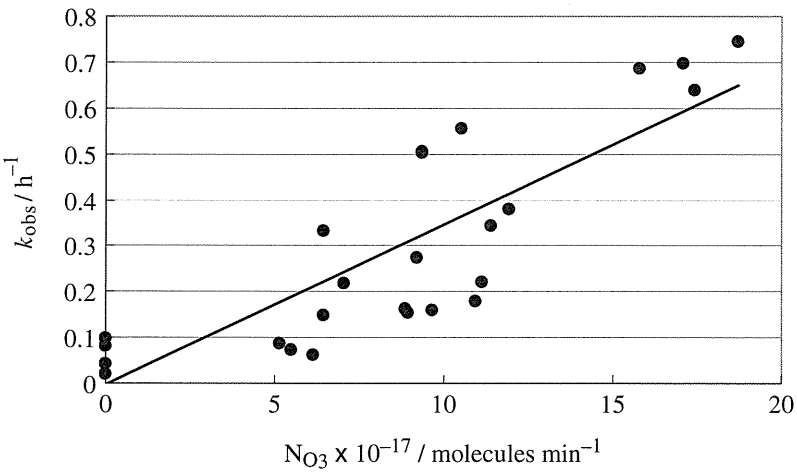

Figure 8. Observed pseudo-first-order rate constants (k_{obs}) for reactions of O_3 with 3-OHNP-d_8 adsorbed on airborne particles plotted against the number of O_3 molecules passing through the quartz fibre filter per minute (N_{O3}/molecules min^{-1}). k_{obs} is expressed as a function of N_{O3}; $k_{obs} = 0.034$ ($N_{O3} \times 10^{-17}$) -0.003. The slope of the regression line has an error of $\pm 6\%$.

constants for the decomposition reactions at several O_3 concentrations. The pseudo-first-order rate constants k_{obs} obtained from the logarithmic plot of the remaining 3-OHNP-d_8 with the exposure time in the present study were plotted versus N_{O3} in Figure 8, clearly highlighting that the k_{obs} values were proportional to N_{O3} ($k_{obs} = 0.034$ ($N_{O3} \times 10^{-17}$) $- 0.003$, $r^2 = 0.73$, $p < 0.01$). Perraudin *et al.* [23] also showed that a similar proportional relationship between the pseudo-first-order rate constants for PAHs decay and the O_3 concentrations exists. Donaldson *et al.* [24] reported that the reaction of PAHs with O_3 on the surface of organic substrates is consistent with a Langmuir-Hinshelwood surface mechanism. The dependence of the pseudo-first-order rate constants k on the gas-phase O_3 concentration is given by

$$k = A[O_3(g)]/(B + [O_3(g)])$$

where A is the product of the maximum number of surface sites available to O_3 and the second-order rate constant for the reaction of PAH with O_3, and B represents the ratio of desorption to adsorption rate constants of O_3. This equation indicates that k exhibits a linear dependence versus the gas-phase O_3 concentration under the $[O_3] \ll B$ condition. Kahan *et al.* [25] showed that the constants B for various PAHs are calculated to be $\sim 10^{15}$ molecules cm^{-3} for the reaction with O_3 on the surface of organic films, which is significantly higher than the ambient O_3 concentration ($\sim 10^{12}$ molecules cm^{-3}). From the linear least-squares fitting line between k_{obs} and N_{O3} obtained in Figure 8, the k_{obs} under any N_{O3} condition can be predicted.

The residual fraction of 3-OHNP-d_8 on a QFF, y (%), after exposure to ambient air under high volume air sampling is expressed as the following equation:

$$y = 100e^{-k_{obs}t} \quad (1)$$

where t is the exposure time. Therefore, assuming that the atmospheric concentration of OHNP is constant during the sample collection, the total ratio of remaining fraction R

Table 1. Atmospheric concentrations of hydroxy-1-nitropyrenes, 1-nitropyrene, and O_3 during 26–27 November 2001 at Sakai, Osaka, Japan.

Compounds	Mean ($n=8$)	Range
3-OHNP[a]	5	2–12[c]
6-OHNP[a]	42	17–73[c]
8-OHNP[a]	50	28–85[c]
1-NP[a]	27	9–48
O_3[b]	27	20–35

Notes: OHNP = hydroxy-1-nitropyrene; 1-NP = 1-nitropyrene.
[a]Given in units of fmol m^{-3}.
[b]Given in units of ppbv. Concentration was revalued to a 3-hour mean, which is coincident with the sampling period of airborne particles.
[c]Each 3-hour mean concentration has an error derived from the error of the slope of the linear regression line in Figure 8. See the caption of Figure 8 for details.

to decomposed fraction D from $t=0$ to $t=T$ is given by:

$$R/D = \left(\int_0^T 100e^{-K_{obs}t}\,dt\right)/\left(100T - \int_0^T 100e^{-K_{obs}t}\,dt\right). \quad (2)$$

It is possible to determine the concentrations of OHNPs in the airborne particles before decomposition by the correction based on this relationship.

The concentrations of 3-, 6-, and 8-OHNPs in airborne particles collected on the QFF at Sakai, Osaka, Japan were determined using the correction method proposed in this study. The mean concentrations of atmospheric 3-, 6-, and 8-OHNPs were 5, 42 and 50 fmol m^{-3} on 26–27 November 2001, respectively (Table 1). The mean measured values of 3-, 6-, and 8-OHNPs before the correction, 3, 25, and 29 fmol m^{-3}, respectively, were ca. 60% of the corrected concentrations. The mean concentration of 1-NP in the airborne particles was 27 fmol m^{-3} on the same sampling day, lower than those of 6- and 8-OHNPs. Gibson *et al.* [4] reported that the atmospheric concentration of OHNPs at a remote site on Bermuda was much higher than that of 1-NP, which is generally emitted from combustion sources. Our result is consistent with this study. These observations suggest that atmospheric secondary formation processes are operating as an atmospheric source of OHNPs. It is critical to clarify the atmospheric occurrence of OHNPs including their sources and sinks to evaluate their health impact on humans.

5. Conclusion

A correction method for the determination of atmospheric OHNPs based on their degradation rates during high volume air sampling was established. The degradation rate constants of OHNPs were found to correlate with the number of ozone molecules passing through the quartz fibre filter in a unit time during high volume air sampling. The chemical loss of OHNPs under high volume air sampling conditions was successfully evaluated by the exposure time and the pseudo-first-order rate constant for OHNP degradation estimated from the correlation. Concentrations of 3-, 6-, and 8-OHNPs in airborne particles collected in Osaka, Japan were determined using the established

correction method, and were comparable to that of 1-NP, a representative atmospheric NPAH.

References

[1] D. Schuetzle, T.L. Riley, T.J. Prater, T.M. Harvey, and D.F. Hunt, Anal. Chem. **54**, 265 (1982).
[2] J.A. Sousa, J.E. Houck, J.A. Cooper, and J.M. Daisey, J. Air Pollut. Control Assoc. **37**, 1439 (1987).
[3] T. Kameda, A. Akiyama, A. Toriba, C. Tachikawa, M. Yoshita, N. Tang, and K. Hayakawa, J. Health. Sci. **54**, 118 (2008).
[4] T.L. Gibson, P.E. Korsog, and G.T. Wolff, Atmos. Environ. **20**, 1575 (1986).
[5] J. Peters and B. Seifert, Atmos. Environ. **14**, 117 (1980).
[6] J.N. Pitts Jr., H.-R. Paur, B. Zielinska, J. Arey, A.M. Winer, T. Ramdahl, and V. Mejia, Chemosphere **15**, 675 (1986).
[7] A.K. Bertram, A.V. Ivanov, M. Hunter, L.T. Molina, and M.J. Molina, J. Phys. Chem. A **105**, 9415 (2001).
[8] C. Schauer, R. Niessner, and U. Pöschl, Environ. Sci. Technol. **37**, 2861 (2003).
[9] D. Grosjean, Atmos. Environ. **17**, 2565 (1983).
[10] M. Tsapakis and E.G. Stephanou, Atmos. Environ. **37**, 4935 (2003).
[11] Y. Liu, M. Sklorz, J. Schnelle-Kreis, J. Orasche, T. Ferge, A. Kettrup, and R. Zimmermann, Chemosphere **62**, 1889 (2006).
[12] D. Schuetzle, Environ. Health Perspect. **47**, 65 (1983).
[13] R. Simo, J.O. Grimalt, and J. Albaiges, Environ. Sci. Technol. **31**, 2697 (1997).
[14] L.M. Ball, M.J. Kohan, L.D. Claxton, and J. Lewtas, Mutat. Res. **138**, 113 (1984).
[15] P.C. Howard, F.A. Beland, and C.E. Cerniglia, Carcinogenesis **4**, 985 (1983).
[16] K.W. Sigvardson, J.M. Kennish, and J.W. Birks, Anal. Chem. **56**, 1096 (1984).
[17] K.W. Sigvardson and J.W. Birks, J. Chromatogr. **316**, 507 (1984).
[18] A. Hartung, J. Kraft, J. Schulze, H. Kieß, and K.-H. Lies, Chromatographia **19**, 269 (1984).
[19] K. Hayakawa, C. Lu, S. Mizukami, A. Toriba, and N. Tang, J. Chromatogr. A **1107**, 286 (2006).
[20] C.-H. Wu, I. Salmeen, and H. Niki, Environ. Sci. Technol. **18**, 603 (1984).
[21] U. Pöschl, T. Letzel, C. Schauer, and R. Niessner, J. Phys. Chem. A **105**, 4019 (2001).
[22] R.M. Kamens, Z. Guo, J.N. Fulcher, and D.A. Bell, Environ. Sci. Technol. **22**, 103 (1988).
[23] E. Perraudin, H. Budzinski, and E. Villenave, J. Atmos. Chem. **56**, 57 (2007).
[24] D.J. Donaldson, B.T. Mmereki, S.R. Chaudhuri, S. Handley, and M. Oh, Faraday Discuss. **130**, 227 (2005).
[25] T.F. Kahan, N.-O.A. Kwamena, and D.J. Donaldson, Atmos. Environ. **40**, 3448 (2006).

Toxic effect of polycyclic aromatic hydrocarbon metabolites on fish bone metabolism

K. Hayakawa[1], N. Suzuki[2], K. Kitamura[3], K. Bekki[1], J. Nakano[1], M. Yoshita[1], A. Toriba[1], T. Kameda[1] & N. Tang[1]
[1]*Institute of Medical, Pharmaceutical and Health Sciences, Kanazawa University, Japan*
[2]*Noto Marine Laboratory, Kanazawa University, Japan*
[3]*Division of Health Sciences, Graduate School of Medical Science, Kanazawa University, Japan*

Abstract

Marine water is contaminated with polycyclic aromatic hydrocarbons (PAHs) from rivers and the atmosphere. Oil spilled from tankers or petroleum factories also causes marine pollution with PAHs. It is well known that PAHs, such as benzo[*a*]pyrene, show carcinogenicity and/or mutagenicity. In developing teleost fish, furthermore, it has been reported that spinal deformity was induced in Pacific herring and pink salmon by PAHs, although the detail mechanism of toxicity in teleosts is not elucidated yet. As a toxic pathway of PAHs in animals, the metabolic activation of PAHs in the presence of P450 is considered. In teleosts, as well as in mammals, it has been reported that PAHs are converted into monohydroxylated polycyclic aromatic hydrocarbons (OHPAHs) by an enzyme: cytochrome P4501A1. Thus, OHPAH might have a toxic effect in teleosts. In the present study, we examined the estrogenic activity of OHPAHs using the yeast-two hybrid assay system with human estrogen receptor (ER) α. As a result, we detected estrogenic activity in 4-hydroxybenz[*a*]anthracene (4-OHBaA). Then, the direct effect of 4-OHBaA on osteoclasts and osteoblasts in teleosts was examined using the assay system with fish scales, which contain osteoclasts, osteoblasts, and the bone matrix of two layers (bony layer: a thin, well-calcified external layer; a fibrillary layer: a thick, partially calcified layer). When the scales of goldfish and wrasse were incubated with 4-OHBaA, which

WIT Transactions on Ecology and the Environment, Vol 135, © 2010 WIT Press
www.witpress.com, ISSN 1743-3541 (on-line)
doi:10.2495/WP100201

showed agonistic activity in the yeast-two hybrid assay system described above, the suppressing effect was observed for both osteoclasts and osteoblasts. The osteoclastic and osteoblastic activities did not change with 1-hydroxypyrene, which has no binding activity to human ERα. Thus, we conclude that PAH metabolites have a toxic effect on fish bone metabolism and that careful attention should be given to aquatic PAH contamination.

Keyword: polycyclic aromatic hydrocarbons, oil spill, yeast-two hybrid assay, osteoclasts, osteoblasts, teleost scale.

1 Introduction

Polycyclic aromatic hydrocarbons (PAHs) are ubiquitous environmental pollutants. They are formed through incomplete combustion of fossil fuel, wood and other organic materials including automobile exhaust, domestic heating and industrial processes.

Storm water runoff and atmospheric deposition of PAHs are now the largest sources of aquatic PAH contamination [1, 2]. Furthermore, an oil spill from an oil tanker, such as the Exxon Valdez and Nakhodka, directly induces contamination by PAHs in a marine environment [3-5]. In the Nakhodka C-heavy oil, 210 μg/g of benz[*a*]anthracene having four aromatic rings was detected [5]. In developing teleosts, it has been reported that spinal deformity was induced in Pacific herring and pink salmon by PAHs [6, 7] although the detail mechanism of toxicity in teleosts has not elucidated yet. As a toxic pathway of PAHs in animals, the metabolic activation of PAHs in the presence of P450 is considered. In teleost fish, as well as in mammals, it is known that PAHs are converted into monohydroxylated polycyclic aromatic hydrocarbons (OHPAHs) by the enzyme cytochrome P4501A1 [7-10]. Thus, PAH metabolites such as OHPAH might have a toxic in teleosts.

In the present study, we examined estrogenic activity of OHPAHs using the yeast-two hybrid assay system with human estrogen receptor (ER) α. Then, the direct effect of 4-hydroxybenz[*a*]anthracene (4-OHBaA) on osteoclasts and osteoblasts in teleosts was examined using the assay system with fish scale, which contains osteoclasts, osteoblasts, and the bone matrix of two layers (bony layer: a thin, well-calcified external layer; a fibrillary layer: a thick, partially calcified layer) [11, 12]. Using the scale assay, furthermore, we compared the results with those of 1-hydroxypyrene (1-OHPy), which had no binding activity to ERα as a negative control.

2 Methods

2.1 Chemicals

Chemical structures of OHPAHs, quinoid PAHs (PAHQs) PAH ketones (PAHKs) and tested in this report are shown in Figs. 1 and 2. These chemicals were purchased from Kanto Chemical (Tokyo, Japan), Aldrich (Milwaukee, WI.

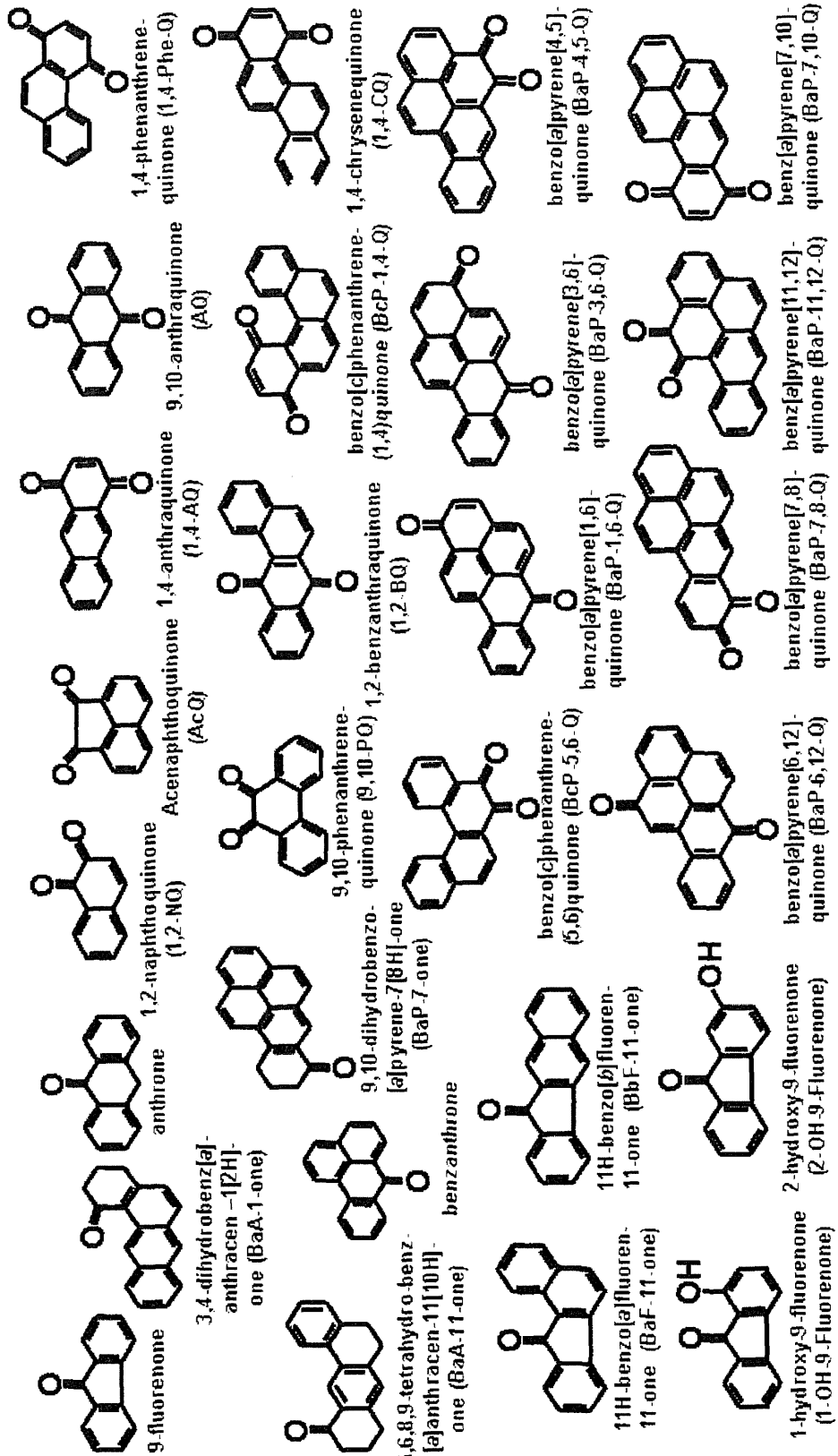

Figure 1: Chemical structures of OHPAHs.

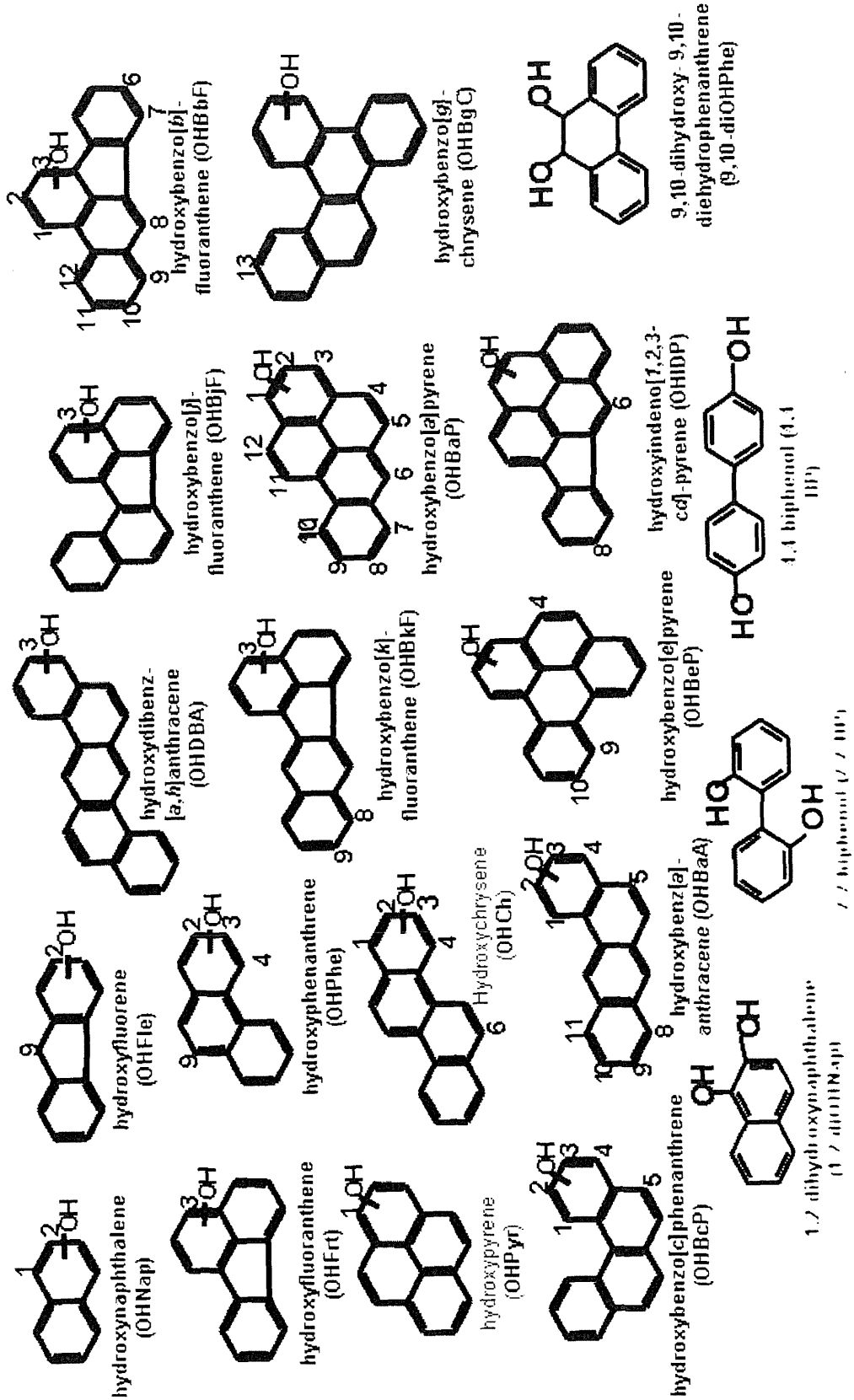
hydroxynaphthalene (OHNap)
hydroxyfluorene (OHFle)
hydroxydibenz-[a,h]anthracene (OHDBA)
hydroxybenzo[b]-fluoranthene (OHBbF)
hydroxyfluoranthene (OHFrt)
hydroxyphenanthrene (OHPhe)
hydroxybenzo[k]-fluoranthene (OHBkF)
hydroxybenzo[j]-fluoranthene (OHBjF)
hydroxypyrene (OHPyr)
Hydroxychrysene (OHCh)
hydroxybenzo[e]pyrene (OHBeP)
hydroxybenzo[g]-chrysene (OHBgC)
hydroxybenzo[c]phenanthrene (OHBcP)
hydroxybenz[a]-anthracene (OHBaA)
hydroxybenzo[a]pyrene (OHBaP)
hydroxyindeno[1,2,3-cd]-pyrene (OHIDP)
9,10-dihydroxy-9,10-diehydrophenanthrene (9,10-diOHPhe)
4,4 biphenol (4,4 BP)

USA), Chiron AS (Trondheim, Norway), and NCI Chemical Carcinogen Repository (Kansas City, MO, USA). Test compounds were dissolved in ethanol and stored at -20°C until use. All other chemicals were of the highest quality available from commercial sources.

2.2 Assay of estrogenic activities

Yeast cells expressing human ERα were prepared according to the previous report [13]. Estrogenic activity of OHPAHs was evaluated by the yeast two-hybrid assay method using the above yeast cells as described [14]. To examine the agonistic activity of OHPAHs, the yeast cells were grown overnight at 27°C with shaking in synthetic defined medium free from tryptophan and leucine, and treated with each test compound in the concentration range from 1×10^{-9} M to 1×10^{-6} M at 27°C for 4 hrs. After the incubation, the treated cells were collected and enzymatically digested with 1 mg/ml Zymolyase 20T at 37°C for 20 min. 2-Nitrophenyl-β-D-galactoside (ONPG) was added to the lysate to a final concentration of 4 mg/ml. After incubation at 27°C for 20 min, the reaction was stopped by the addition of 1 M Na_2CO_3. The yeast debris was removed by centrifugation and β-galactosidase activity was assayed by measuring the absorbance of supernatant at 415 nm. Three independent experiments were run, and the mean values of the three were shown in this report. Relative effective potency of estrogenic activity (REP_E) was calculated as the value of the relative concentration of the test compound that gave the same activity of 17β-estradiol (E_2).

2.3 Animals

A previous study [15] indicated that sensitivity to calcemic hormones was higher in mature female than in mature male teleosts. Therefore, female goldfish (*Carassius auratus*) were purchased from a commercial source (Higashikawa Fish Farm, Yamato-koriyama, Japan), and their scales were used in an *in vitro* assay. As a marine teleost, female wrasse (*Pseudolabrus sieboldi*) caught in Tsukumo Bay of Noto Peninsula were used. These fish were kept under normal conditions until the start of experiments.

All experimental procedures were conducted in accordance with the Guide for the Care and Use of Laboratory Animals of Kanazawa University.

2.4 Effects of OHPAHs and E_2 on osteoclastic activity in cultured scales of goldfish and wrasse

The 4-OHBaA and 1-OHPy (NCI Chemical Carcinogen Repository), and E_2 (water-soluble type, Sigma-Aldrich, Inc., MO, USA) were purchased and used in the present study.

A 1% penicillin-streptomycin mixture (ICN Biomedicals, Inc., OH, USA) was added to Eagle's modified minimum essential medium (MEM; ICN Biomedicals, Inc.). HEPES (Research Organics, Inc., OH, USA) (20 mM) was added to MEM and adjusted to pH 7.0. After filtration, MEM was used in this experiment. Scales were collected from goldfish and wrasse under anesthesia

with ethyl 3-aminobenzoate, methanesulfonic acid salt (Sigma-Aldrich, Inc.). The scales were cut into halves. One half of a piece was then placed into a well of a 24-well microplate in MEM (1 ml) supplemented with OHPAHs or E_2 (10^{-7}, 10^{-6}, and 10^{-5} M). The other half was also placed into a well of a 24-well microplate in an OHPAH/E_2-free medium as a control. Eight scales were used for each dose. These scales were incubated for 6 hrs at 15°C. After incubation, each incubated scale was washed with saline and transferred to its own well in a 96-well microplate. An aliquot of 100 µl of 20 mM tartrate in a 0.1 M sodium acetate buffer (pH 5.3) was added to each well. This microplate was frozen at -85°C immediately and kept at -20°C until analysis.

To analyze the tartrate-resistant acid phosphatase (TRAP) activity, an aliquot of 100 µl of 20 mM para-nitrophenyl-phosphate and 20 mM tartrate in a 0.1 M sodium acetate buffer (pH 5.3) was added to each well of a melted solution in the microplate. This plate was incubated at 20°C for 30 min while being shaken. After incubation, the reaction was stopped by adding 50 µl of a 3 N NaOH-20 mM EDTA solution. A colored solution of 150 µl was transferred to a new plate, and the absorbance was measured at 405 nm. The absorbance was converted into the amount of produced para-nitrophenol (pNP) using a standard curve for pNP. Detail methods were described in Suzuki *et al.* [11].

2.5 Effects of OHPAHs and E_2 on osteoblastic activity in cultured scales of goldfish and wrasse

Goldfish and wrasse were anesthetized with ethyl 3-aminobenzoate, methanesulfonic acid salt (Sigma-Aldrich, Inc.), and scales were collected from them. The scales were cut into halves. One half of a piece was then placed into a well of a 24-well microplate in MEM (1 ml) supplemented with OHPAHs or E_2 (10^{-7}, 10^{-6}, and 10^{-5} M). The other half was also placed into a well of a 24-well microplate as a control. Eight scales were used for each dose. These scales were incubated for 6 hrs at 15°C. After incubation, each incubated scale was washed with saline and transferred to its own well in a 96-well microplate. An aliquot of 100 µl of an alkaline buffer (100 mM Tris-HCl, pH 9.5; 1 mM $MgCl_2$; 0.1 mM $ZnCl_2$) was added to each well. This microplate was frozen at -85°C immediately and kept at -20°C until analysis.

The ALP activities were measured in the same manner as for the measurement of TRAP activity.

2.6 Statistical analysis

The statistical significance was assessed by the student's *t*-test. The selected significance level was $P < 0.05$.

3 Results

3.1 Estrogenic activity

The results are indicated in Figure 3. A significant increase of β-galactosidase activity ($REP_E > 1 \times 10^{-3}$) was observed for 3-, 4- and 10-OHBaAs and

2-hydroxychrysene (2-OHCh). These were all 4-ring OHPAHs. Among them, 4-OHBaA exhibited the strongest estrogenic activity (REP_E = 7.5 × 10^{-3}). 2-hydroxyfluorene (2-OHFle), 2-hydroxuphenanthrene (2-OHPh) (3-ring), 3-hydroxyfluoranthene (3-OHFrt), 1-OHPy, 1-OHCh, 3-hydroxybenzo[*k*]fluoranthene, 12-hydroxybenzo[*b*]fluoranthene (4-ring) and 4-hydroxybenzo[*e*]pyrene (5-ring) were also active ($1 \times 10^{-3} > REP_E \geq 1 \times 10^{-4}$). The estrogenic activities of the other OHPAHs, PAHQs and PAHKs were much weaker or undetectable.

3.2 Effects of OHPAHs and E_2 on osteoclastic activity in cultured scales of goldfish and wrasse

The results are summarized in Table 1. In goldfish, the TRAP activity of the scales was significantly lowered by 4-OHBaA treatment at 6 hrs of incubation (10^{-7} and 10^{-6} M, $P < 0.05$, 10^{-5} M, $P < 0.01$), although the TRAP activity did not change from that of the control with 1-OHPy. E_2 significantly increased the TRAP activity at 6 hrs (10^{-6} and 10^{-5} M, $P < 0.05$).

In the scales of wrasse after 4-OHBaA (10^{-7} to 10^{-5} M) treatment, the TRAP activity also decreased at 6 hrs (10^{-6} M, $P < 0.05$, 10^{-5} M, $P < 0.01$). There was no change in the TRAP activity in 1-OHPy-treated scales. In wrasse as well as goldfish, a significant difference (10^{-5} M, $P < 0.01$) was obtained between E_2-treated scales and control scales.

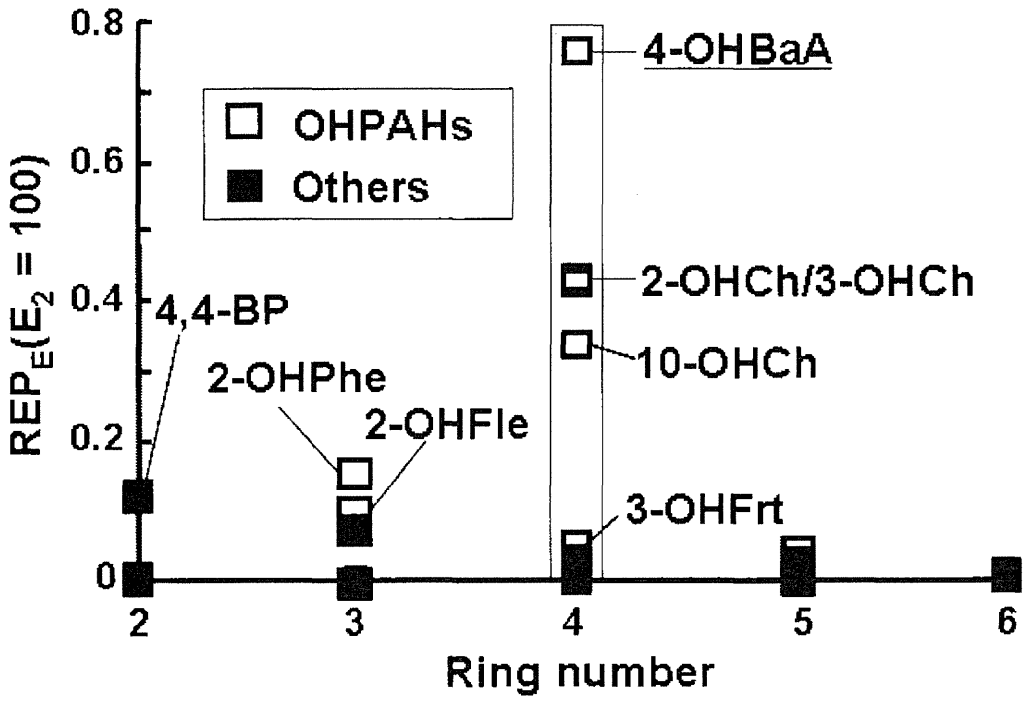

Figure 3: Relationship between the number of rings of OHPAHs and REP_E. REP_E indicates the relative effective potency of estrogenic activity.

Table 1: The toxicity of 4-OHBaA in osteoclasts and osteoblasts of the scales.

Goldfish (Fresh water teleost)	Osteoclasts	Osteoblasts
4-OHBaA	inhibition (10^{-7} M)	inhibition (10^{-5} M)
E_2	activation (10^{-6} M)	activation (10^{-6} M)
1-OHPy	no change	no change
Wrasse (Seawater teleost)		
4-OHBaA	inhibition (10^{-6} M)	inhibition (10^{-5} M)
E_2	activation (10^{-5} M)	activation (10^{-5} M)
1-OHPy	no change	no change

4-OHBaA: 4-hydroxybenz[*a*]anthracene
E_2: 17β-estradiol
1-OHPy: 1-hydroxypyrene

3.3 Effects of OHPAHs and E_2 on osteoblastic activity in cultured scales of goldfish and wrasse

The results are summarized in Table 1. In goldfish scales, at 6 hrs of incubation, the alkaline phosphatase (ALP) activity significantly decreased from the control values as a result of 4-OHBaA treatment (10^{-5} M, $P < 0.01$), while the ALP activity did not change with 1-OHPy treatment. E_2 significantly increased the ALP activity at 6 hrs of incubation (10^{-6} M, $P < 0.01$; 10^{-5} M, $P < 0.05$).

Similar changes were induced by 4-OHBaA in the scales of wrasse. The ALP activity significantly decreased in 4-OHBaA-treated wrasse scales at 6 hrs (4-OHBaA: 10^{-5} M, $P < 0.01$), although the ALP activity did not change from that of the control with 1-OHPy. In wrasse, a significant difference (at 6 hrs: 10^{-5} M, $P < 0.01$) was obtained between E_2-treated scales and control scales.

4 Discussion

The present study indicates that OHPAHs such as 4-OHBaA have an estrogenic activity using the yeast-two hybrid assay system with human ERα. In rat cytosol as well, 2-hydroxybenz[*a*]anthracene bound strongly to ER [16]. In the ERα reporter assay using a human breast cancer cell line (MCF-7), 3-OHBaA and 9-OHBaA had binding activity to ER [8]. Our data are supported by these reports.

In both freshwater and seawater teleosts, 4-OHBaA suppressed both osteoclastic and osteoblastic activities in the scales using our *in vitro* assay system while E_2 activated both osteoclastic and osteoblastic activities in the scales. E_2-specific binding [17] was detected in the scales of rainbow trout. However, a different action from E_2-treated scales was obtained in OHPAH-

treated scales. In the case of bisphenol-A, which is bound to mammalian ERα [18], we previously reported that both osteoclastic and osteoblastic activities in the goldfish scales were significantly suppressed by bisphenol-A treatment [19]. In bony tissues including the scale of teleost, the β subtype of the ER is mainly expressed [20], while α subtype of ER is expressed in mammals [8]. This may be one reason for the anti-estrogenic-like action in OHPAH. To examine the effects of OHPAHs on bone tissues of teleosts in detail, plans are underway to conduct micro-array analyses using the scales of zebrafish.

The present study indicated that the strength of the inhibition activity in goldfish was stronger than that in wrasse. In goldfish, even at 10^{-7} M of 4-OHBaA, the osteoclastic activity was significantly inhibited. Exchange of calcium in the scales of freshwater teleosts may be faster than that in marine teleosts because they live in a low-calcium environment. In fact, the response of estrogen and calcitonin in the scales of freshwater teleosts was higher than that in those of marine teleosts [15, 21-23]. In the case of the scales, therefore, OHPAHs were more toxic in freshwater teleosts.

An oil spill from an oil tanker such as the Exxon Valdez and Nakhodka directly induces contamination by PAHs in a marine environment. In the C-heavy oil of the Nakhodka, 210 μg/g of BaA having four aromatic rings was detected [5]. This concentration is similar to that in the present experiment. Immediately after the oil spill, the high level of PAHs influenced marine animals, including fish. For a long time (more than 14 years), the toxicity of PAHs originating from an oil spill affected many marine animals (for a review, see Peterson *et al.* [24]). These facts, in conjunction with the findings of our study, indicate that careful attention should be given to aquatic PAH contamination.

5 Conclusion

We found that OHPAHs such as 4-OHBaA had an estrogenic activity using the yeast-two hybrid assay system with human ERα. This chemical suppressed both osteoclastic and osteoblastic activity in the scales of both freshwater and seawater teleosts. We believe that these phenomena are a cause of the disruption of the bone metabolism and the induction of spinal deformities in teleosts.

Acknowledgements

This study was supported in part by grants to K. Hayakawa (Grant-in-Aid for Scientific Research of ExTEND2005 and Global Environment Research Fund D-091 by the Ministry of Environment in Japan; Grant-in-Aid for Scientific Research (B) No. 21390034 and for Exploratory Research No.21651018 by Japan Society for the Promotion of Science), to N. Suzuki (Kurita Water and Environment Foundation; Grant-in-Aid for Scientific Research (C) No. 21500404 by JSPS), and to K. Kitamura (Grant-in-Aid for Scientific Research (C) No. 21500681 by JSPS).

References

[1] Lima, A. L. C., Eglinton, T. I. & Reddy, C. M., High-resolution record of pyrogenic polycyclic aromatic hydrocarbon deposition during the 20th century. *Environmental Science and Technology*, **37**, pp.53-61, 2003.

[2] Li, D. & Daler, D., Ocean pollution from land-based sources: East China Sea, China. *Ambio*, **33**, pp.107 113, 2004.

[3] Bue, B. G., Sharr, S. & Seeb, J. E., Evidence of damage to pink salmon populations inhabiting Prince William Sound, Alaska, two generations after the Exxon Valdez oil spill. *Transactions of the American Fisheries Society*, **127**, pp. 35-43, 1998.

[4] Heintz, R. A., Rice, S. D., Wertheimer, A. C., Bradshaw, R. F., Thrower, F. P., Joyce, J. E. & Short, J. W., Delayed effects on growth and marine survival of pink salmon *Oncorhynchus gorbuscha* after exposure to crude oil during embryonic development. *Marine Ecology Progress Series*, **208**, pp. 205-216, 2000.

[5] Hayakawa, K., Nomura, M., Nakagawa, T., Oguri, S., Kawanishi, T., Toriba, A., Kizu, R., Sakaguchi, T. & Tamiya, E., Damage to and recovery of coastlines polluted with C-heavy oil spilled from the Nakhodka. *Water Research*, **40**, pp. 981-989, 2006.

[6] Barron, M. G., Carls, M. G., Heintz, R. & Rice, S. D., Evaluation of fish early life-stage toxicity models of chronic embryonic exposures to complex polycyclic aromatic hydrocarbon mixtures. *Toxicological Science*, **78**, pp. 60-67, 2004.

[7] Billiard, S. M., Timme-Laragy, A. R., Wassenberg, D. M., Cockman, C. & Di, Giulio, R. T., The role of the aryl hydrocarbon receptor pathway in mediating synergistic developmental toxicity of polycyclic aromatic hydrocarbons to zebrafish. *Toxicological Sciences*, **92**, pp. 526-536, 2006.

[8] Charles, G. D., Bartels, M. J., Zacharewski, T. R., Gollapudi, B. B., Freshour, N. L. & Carney, E. W., Activity of benzo[*a*]pyrene and its hydroxylated metabolites in an estrogen receptor-α reporter gene assay. *Toxicological Sciences*, **55**, pp. 320-326, 2000.

[9] Jaruchotikamol, A., Jarukamjorn, K., Sirisangtrakul, W., Sakuma, T., Kawasaki, Y. & Nemoto, N., Strong synergistic induction of CYP1A1 expression by andrographolide plus typical CYP1A inducers in mouse hepatocytes. *Toxicology and Applied Pharmacology*, **224**, pp. 156-162, 2007.

[10] Mortensen, A. S. & Arukwe, A., Targeted salmon gene array (SalArray): A toxicogenomic tool for gene expression profiling of interactions between estrogen and aryl hydrocarbon receptor signaling pathways. *Chemical Research in Toxicology*, **20**, pp. 474-488, 2007.

[11] Suzuki, N., Kitamura, K., Nemoto, T., Shimizu, N., Wada, S., Kondo, T., Tabata, M. J., Sodeyama, F., Ijiri, K. & Hattori, A., Effect of vibration on osteoblastic and osteoclastic activities: Analysis of bone metabolism using goldfish scale as a model for bone. *Advance in Space Research*, **40**, pp. 1711-1721, 2007.

[12] Suzuki, N., Somei, M., Seki, A., Reiter, R. J. & Hattori, A., Novel bromomelatonin derivatives as potentially effective drugs to treat bone diseases. *Journal of Pineal Research*, **45**, pp. 229 234, 2008.
[13] Morito, K., Hirose, T., Kinjo, J., Hirakawa, T., Okawa, M., Nohara, T., Ogawa, S., Muramatsu, M. & Masamune, Y., Interaction of phytoestrogen with estrogen receptor α and β. *Biol. Pharm. Bull.*, **24**, pp. 351-356, 2001.
[14] Hirose, T., Morito, K., Kizu, R., Toriba, A., Hayakawa, K., Ogawa, S., Inoue, S., Muramatsu, M. & Masamune, Y., Estrogenic/antiestrogenic activities of benzo[*a*]pyrene monohydroxy derivatives. *Journal of Health Science*, **47**, pp. 552-558, 2001.
[15] Suzuki, N., Suzuki, T. & Kurokawa, T., Suppression of osteoclastic activities by calcitonin in the scales of goldfish (freshwater teleost) and nibbler fish (seawater teleost). *Peptides*, **21**, pp. 115-124, 2000.
[16] Ebright, R. H., Wong, J. R. & Chen, L. B., Binding of 2-hydroxybenzo[*a*]pyrene to estrogen receptors in rat cytosol. *Cancer Research*, **46**, pp. 2349-2351, 1986.
[17] Persson, P., Shrimpton, J. M., McCormick, S. D. & Björnsson, B. Th., The presence of high-affinity, low-capacity estradiol-17β binding in rainbow trout scale indicates a possible endocrine route for the regulation of scale resorption. *General and Comparative Endocrinology*, **120**, pp. 35-43, 2000.
[18] Singleton, D. W., Feng, Y., Yang, J., Puga, A., Lee, A. V. & Khan, S. A., Gene expression profiling reveals novel regulation by bisphenol-A in estrogen receptor-α-positive human cells. *Environmental research*, **100**, pp. 86-92, 2006.
[19] Suzuki, N. & Hattori, A., Bisphenol A suppresses osteoclastic and osteoblastic activities in the cultured scales of goldfish. *Life Sciences*, **73**, pp. 2237-2247, 2003.
[20] Yoshikubo, H., Suzuki, N., Takemura, K., Hoso, M., Yashima, S., Iwamuro, S., Takagi, Y., Tabata, M. J. & Hattori, A., Osteoblastic activity and estrogenic response in the regenerating scale of goldfish, a good model of osteogenesis. *Life Sciences*, **76**, pp. 2699-2709, 2005.
[21] Persson, P., Sundell, K. & Björnsson, B. Th., Estradiol-17β-induced calcium uptake and resorption in juvenile rainbow trout, *Oncorhynchus mykiss*. *Fish Physiology and Biochemistry*, **13**, pp. 379-386, 1994.
[22] Persson, P., Takagi, Y. & Björnsson, B. Th., Tartrate resistant acid phosphatase as a marker for scale resorption in rainbow trout, *Oncorhynchus mykiss*: Effects of estradiol-17β treatment and refeeding. *Fish Physiology and Biochemistry*, **14**, pp. 329-339, 1995.
[23] Guerreiro, P. M., Fuentes, J., Canario, A. V. M. & Power, D. M., Calcium balance in sea bream (*Sparus aurata*): The effect of oestradiol-17β. *Journal of Endocrinology*, **173**, pp. 377-385, 2002.
[24] Peterson, C. H., Rice, S. D., Short, J. W., Esler, D., Bodkin, J. L., Ballachey, B. E. & Irons, D. B., Long-term ecosystem response to the Exxon Valdez oil spill. *Science*, **302**, pp. 2082-2086, 2003.